

RSC Advances



This is an *Accepted Manuscript*, which has been through the Royal Society of Chemistry peer review process and has been accepted for publication.

Accepted Manuscripts are published online shortly after acceptance, before technical editing, formatting and proof reading. Using this free service, authors can make their results available to the community, in citable form, before we publish the edited article. This *Accepted Manuscript* will be replaced by the edited, formatted and paginated article as soon as this is available.

You can find more information about *Accepted Manuscripts* in the [Information for Authors](#).

Please note that technical editing may introduce minor changes to the text and/or graphics, which may alter content. The journal's standard [Terms & Conditions](#) and the [Ethical guidelines](#) still apply. In no event shall the Royal Society of Chemistry be held responsible for any errors or omissions in this *Accepted Manuscript* or any consequences arising from the use of any information it contains.

Cite this: DOI: 10.1039/c0xx00000x

www.rsc.org/xxxxxx

Communication

Fabrication of TiO₂/MS (M=Pb, Zn) core-shell coaxial nanotube arrays and their photocatalytic properties

Xiaofei Qu,^a Yuchen Hou,^a Chengpeng Wang,^a Fanglin Du^{*a} and Lixin Cao^b

Received (in XXX, XXX) Xth XXXXXXXXXX 20XX, Accepted Xth XXXXXXXXXX 20XX

DOI: 10.1039/b000000x

In this work, TiO₂/MS (M=Pb, Zn) core-shell coaxial nanotube arrays were prepared by a simple method of liquid deposition using anodic aluminium oxide templates. The mechanism of the formation of TiO₂/MS (M=Pb, Zn) coaxial nanotubes was discussed. Compared to bare TiO₂ nanotubes, TiO₂/PbS and TiO₂/ZnS composite nanotubes showed improved photocatalytic properties and analysis of such results was also conducted.

With the development of economy and industry, the sewage drained by factory would seriously harm the environment. The idea using sunlight as driving force for semiconductors to degrade pollutant into nontoxic materials has been more and more popular. Among various of semiconductors, TiO₂ is more attractive because of its amazing characters such as high stability, non-toxicity, high oxidative power and low cost. It has been used widely in many fields such as solar cells, water splitting and degradation of toxic chemicals.¹⁻³ However, due to the wide band gap (3.2eV), the photoresponse of TiO₂ is restricted to only ultraviolet region with the wavelength < 390nm, which significantly diminishes the utilization of solar energy. Therefore, for TiO₂, many methods have been applied to better the performance in optical absorption. Such designed strategies include doping TiO₂ with metal or nonmetal ions,⁴⁻⁵ decorating TiO₂ with quantum dots (QDs),⁶⁻⁷ and coupling TiO₂ with other semiconductors.⁸⁻¹⁰ Among those various semiconductors, PbS and ZnS are two considerable and attractive choices. PbS as a narrow band gap material (0.37eV) has an extended photoresponse region of sunlight. And for ZnS, the potentials of the conduction band and the valence band are both charged a bit more negative than TiO₂. This unique band structure could enhance the separation of the photoproduced holes and electrons. And as we all know, nanotubes own the superiorities of the large surface-to-volume ratios and large surface area compared with bulk materials. Now there has been many works concerning the fabrication of TiO₂ nanotubes: synthesis of TiO₂ nanotubes by anodization of high-pure Ti foils,^{11,12} hydrothermal synthesis,¹³ sol-gel method¹⁴ or solvothermal process.¹⁵ Anodic aluminium oxide (AAO) membrane contains hexagonally ordered porous structure and could be a suitable template for the fabrication of one-dimensional nano-structures. Up to now, there has been some studies about fabricating nano-structures by double diffusion method with the assistance of AAO templates¹⁶⁻¹⁷.

In this study we use AAO membrane (Fig. 1a) as the template

to prepare TiO₂/MS (M=Pb, Zn) core-shell coaxial nanotube arrays. First, fabricate TiO₂ shell (Fig. 1b) on the inwall of AAO template by liquid deposition. Then, precipitate MS (M=Zn, Pb) core (Fig. 1c) on the TiO₂ shell by double diffusion (Fig. 1d) during hydrothermal reaction. Briefly, the AAO template with TiO₂ precursors on it was immersed into separate solutions of Na₂S₂O₃ and M(CH₃COO)₂ (M=Pb, Zn), where the template worked as a septum between the two solutions (Fig. 1d), and the reaction was carried out in teflon-lined at 180°C for 6 hours. Further experimental details are provided in the ESI.† Although there has been some studies on the modifications of TiO₂ with MS (M=Zn, Pb), which mainly focused on fabricating composites of disordered nanoparticles^{18,19} or films²⁰, there are few reports concerning about the PbS, ZnS modified TiO₂ to form a core-shell coaxial composite nanotubes. One of the main purposes of our work is to propose a simple and convenient method to fabricate ordered TiO₂/MS core-shell coaxial composite nanotube arrays, which could also be used to synthesize other kinds of core-shell coaxial composites.

For SEM and TEM tests, the AAO templates were dissolved using NaOH solution and the nanotubes were all free from the templates. For the other tests, the nanotubes were all embedded in the AAO templates. Fig. 2a~f showed the SEM images of the samples. Fig. 2a was the morphology of AAO template, with an average pore diameter of 250nm. Fig. 2b showed that the TiO₂

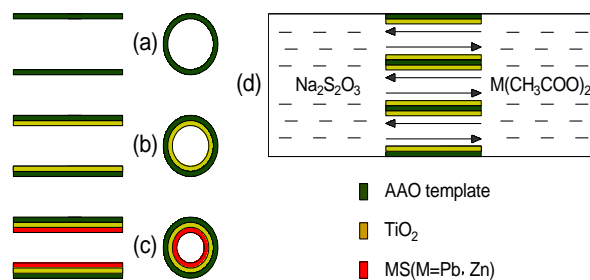


Fig. 1: A simple diagram of the reaction process: (a) a single nanochannel of AAO template; (b) TiO₂ shell was deposited on the inwall of AAO template; (c) MS (M=Pb, Zn) core was fabricated on the inwall of TiO₂ shell; (d) diagram of the double diffusion process during fabrication of MS core.

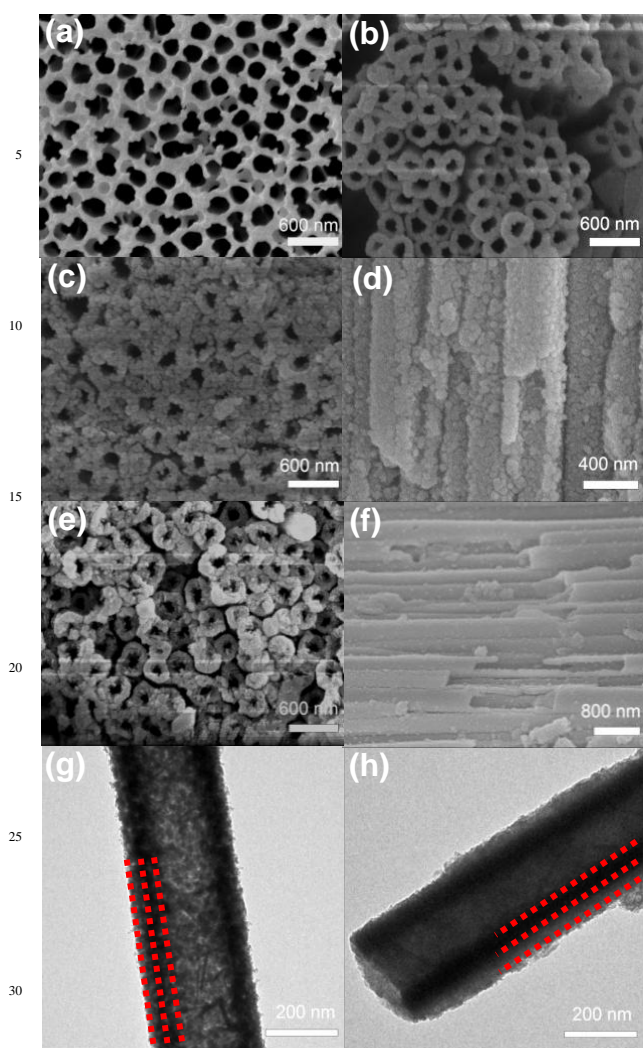


Fig. 2: SEM images of: (a) AAO template; (b) TiO_2 produced by liquid deposition; (c)-(d) TiO_2/PbS core-shell coaxial nanotube arrays; (e)-(f) TiO_2/ZnS core-shell coaxial nanotube arrays and TEM images of: (g) one single TiO_2/PbS core-shell coaxial nanotube; (h) one single TiO_2/ZnS core-shell coaxial nanotube.

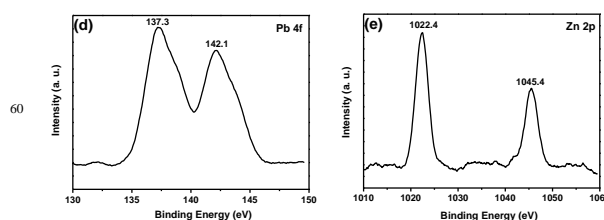
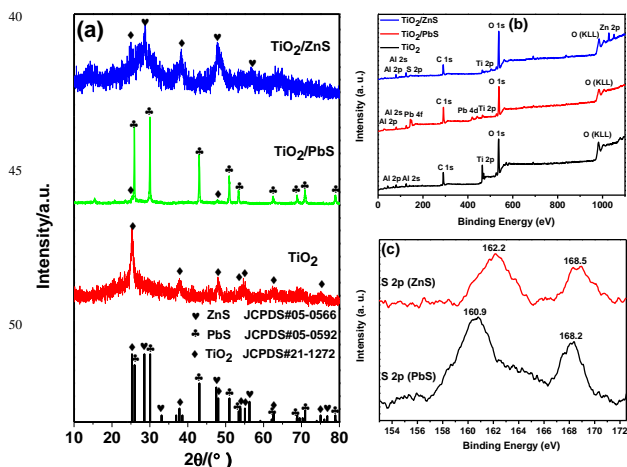


Fig. 3: (a) XRD patterns of TiO_2 , TiO_2/PbS , TiO_2/ZnS nanotube arrays; (b) XPS whole scanning spectrum of TiO_2 , TiO_2/PbS , TiO_2/ZnS nanotube arrays; (c)-(e) High-resolution XPS spectra of S, Pb and Zn.

nanotubes produced by liquid deposition had an average pore diameter of 200nm. Fig. 2c and 2d were the SEM images of TiO_2/PbS nanotubes. From the two images, the pore diameter of TiO_2/PbS nanotubes was $\sim 180\text{nm}$, which was smaller than that of TiO_2 nanotubes. From Fig. 2e and 2f, the hollow structure could also be found for TiO_2/ZnS nanotubes. Similarly, the pore diameter of TiO_2/ZnS nanotubes was obviously smaller than that of TiO_2 nanotubes. So it was safe to say that the MS could be deposited on the inner of TiO_2 nanotubes by means of double diffusion through the AAO template. In order to show the structure of the prepared samples clearly, TEM test was also carried out in this work. From Fig. 2g, we could see that the pore diameter of the TiO_2/PbS nanotube was $\sim 180\text{nm}$, while the thickness of TiO_2 was $\sim 20\text{nm}$ and that of PbS was $\sim 10\text{nm}$. From Fig. 2h, the thickness of TiO_2 shell about 20nm and that of ZnS core about 30nm could also be found. The distinct interface between the outer layer of TiO_2 and the inner layer of MS suggested the structure of core-shell coaxial nanotube were obtained by our simple method.

Fig. 3 exhibited crystal structure, elemental composition and chemical state of the samples. Fig. 3a was the XRD spectra of TiO_2 , TiO_2/PbS , and TiO_2/ZnS nanotube arrays. From the XRD pattern of TiO_2 nanotube arrays, it was clear that TiO_2 was anatase phase with the main peaks at $2\theta=25.3^\circ$, 38.6° , 48.0° , 53.9° , 55.0° , 62.7° , 74.0° corresponding to (101), (112), (200), (105), (211), (204), (107) planes of anatase TiO_2 (JCPD#21-1272), respectively. For TiO_2/PbS NTAs, except for the peaks ($2\theta=25.3^\circ$, 48.0°) from TiO_2 , the peaks at $2\theta=26.0^\circ$, 30.1° , 43.1° , 51.0° , 53.4° , 62.5° , 68.9° , 71.0° , 78.9° corresponding to (111), (200), (220), (311), (222), (400), (331), (420), (422) planes of cubic PbS (JCPDS#05-0592), revealed that the PbS existed in the product. For TiO_2/ZnS NTAs, except for the peaks of TiO_2 , the other peaks located at $2\theta=28.6^\circ$, 47.6° and 56.3° was a good evidence of cubic ZnS (JCPD#05-0566).

The elemental composition and the chemical state of the samples were further investigated by XPS (Fig. 3b-e). The Fig. 3b was the whole scanning spectrum of TiO_2 , TiO_2/PbS , TiO_2/ZnS nanotube arrays, showing the main elemental composition of the samples, including Ti, O, Zn, Pb, S. Here, the XPS peaks of S (2p at 162.2eV for ZnS and 160.9eV for PbS) were in agreement with the binding energy of Zn-S bond and Pb-S bond, respectively (Fig. 3c).^{21,22} The additional peaks of S (2p at 168.5eV for ZnS and 168.2eV for PbS) may arise from residual surface contaminant, for example, $\text{Na}_2\text{S}_2\text{O}_3$.²³ The peaks at 137.3eV and 142.1eV were corresponding to the previously

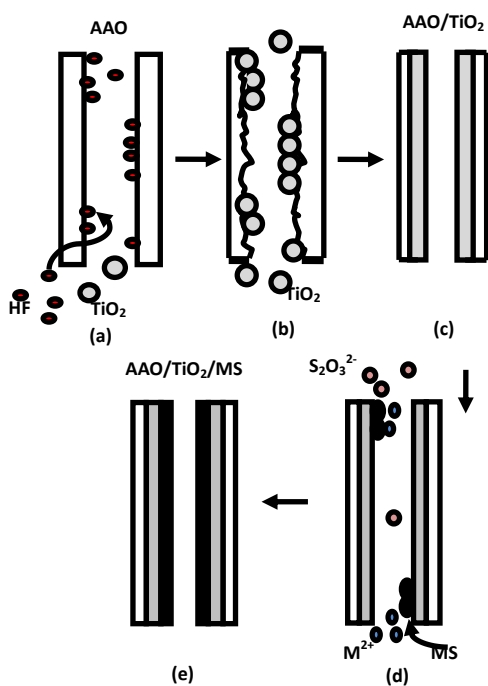


Fig. 4: (a)-(c) Liquid deposition of TiO₂ on the inwall of AAO template; (d)-(e) deposition of MS (M=Pb, Zn) on the inwall of AAO/TiO₂.

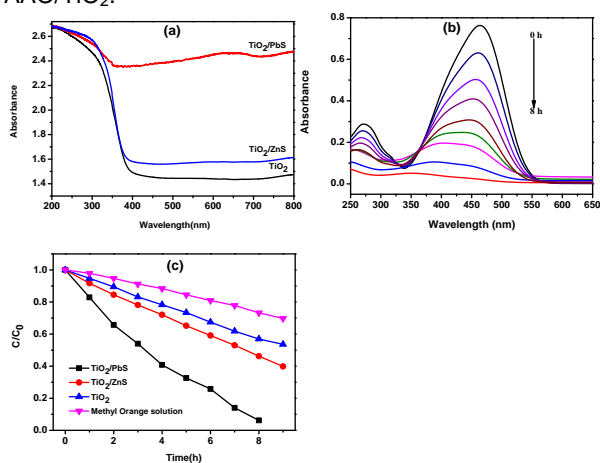
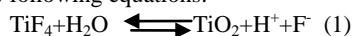


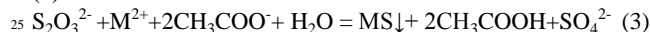
Fig. 5: (a) UV-Vis diffuse-reflectance spectra of TiO₂, TiO₂/PbS, TiO₂/ZnS nanotubes; (b) absorption spectrum of methyl orange in the presence of TiO₂/PbS nanotubes; (c) photocatalytic performance of TiO₂, TiO₂/PbS, TiO₂/ZnS nanotubes for the degradation of methyl orange solution under UV light.

reported binding energy of Pb 4f_{5/2} and 4f_{7/2}, respectively, indicating the presence of Pb²⁺ (Fig. 3d).²⁴ The two strong peaks in Fig. 3e at 1022.4eV and 1045.4eV were assigned to the binding energy of Zn 2p_{3/2} and Zn 2p_{1/2}, respectively, suggesting the existence of Zn²⁺.²⁵ All these results suggested that the ZnS and PbS were obtained in our work.

The mechanism of the formation of TiO₂/MS (M=Pb, Zn) core-shell coaxial nanotubes was shown in Figure 5. The deposition of TiO₂ on the inwall of AAO template could be described by



TiF₄ will be transformed into HF and TiO₂ in the solution (Equation (1)). As a F⁻ trapping agent, Al₂O₃ will consume F⁻ and H⁺ (Reaction (2)). With the Reaction (2) proceeding toward right-hand side, the production of TiO₂ and HF (Fig. 4a) will be boosted. Because HF has an erosion effect on AAO template (Equation (2)), the surface of the nanochannels will become rough and full of bumps and pit, which makes it easy for TiO₂ particles to adhere to (Fig. 4b). Eventually, with the proceeding of the reaction, ordered TiO₂ nanotube arrays could be formed in the AAO template (Fig. 4c). As for the deposition of MS on AAO/TiO₂, it could be explained using the following Reaction (3):



Due to the concentration gradient between the two sides of the AAO/TiO₂ template (septum), S₂O₃²⁻ and M²⁺ will migrate to the opposite side through the nanochannels (Fig. 4d), encounter each other, and finally form the MS sediments on the inwall of AAO/TiO₂. Hereto, the fabrication of TiO₂/MS core-shell coaxial nanotube arrays is finished in the manner of double diffusion (Fig. 4e).

Fig. 5a showed the UV-Vis diffuse-reflectance spectra of the samples. From the spectra, it could be seen that the absorption onset of TiO₂ lied at 387nm, corresponding to that of anatase TiO₂. After coupling with PbS or ZnS, the onset of TiO₂/MS showed a red-shift more or less. Especially, for TiO₂/PbS, it exhibited a significantly enhanced light absorption, covering almost the entire visible region. This character may be helpful for its photocatalytic activity. The photocatalytic activity of TiO₂/PbS core-shell coaxial nanotube arrays measured by the degradation of methyl orange was shown in Fig. 5b. Experimental details about the test of photocatalytic activity are provided in the ESI.† It was clear that there were two obvious absorption peaks at about 280nm and 465nm, corresponding to the absorption peaks of methyl orange.²⁶ The UV-Vis absorption of methyl orange at 465nm was chosen as the parameter for the photocatalytic activity and the peak diminished gradually as the exposure time increased. When the exposure time reached to 8 hours, the peak almost disappeared, indicating that the methyl orange was almost degraded completely. Furthermore, photocatalytic activities of the three samples were illustrated in Fig. 5c. The degradation efficiency of the samples was calculated by C/C₀, where C₀ was the initial concentration of methyl orange, and C was the concentration during the reaction. Although methyl orange showed a little degradation because of the long time under UV light irradiation, among the four samples, the order of their photocatalytic performance was shown as follows: TiO₂/PbS > TiO₂/ZnS > TiO₂ > MO. After coupled with MS, the photocatalytic properties of the TiO₂/MS composite core-shell nanotubes were greatly enhanced than that of bare TiO₂ nanotubes.

Here the better photocatalytic performance of TiO₂/PbS or TiO₂/ZnS than that of TiO₂ could be explained as follows (Fig. 6). As schematized in Fig. 6a, conduct band (CB) of TiO₂ lies at a more negative potential than that of PbS, therefore the excited electrons have a tendency to transfer from CB of TiO₂ to that of PbS. Because of the huge gap (2.3eV) between valance band (VB) of PbS and that of TiO₂, it may be extremely hard for the holes to

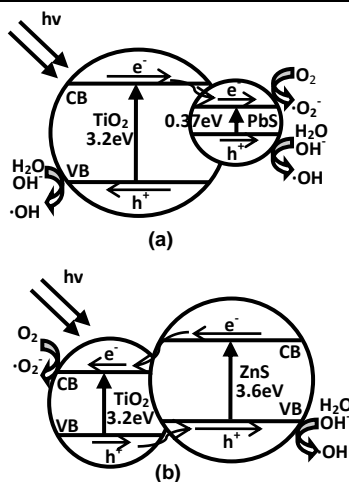


Fig. 6: Schematic illustration of the band structure related photocatalytic mechanism of the TiO₂/PbS(a), TiO₂/ZnS(b) heterostructure.

transit from VB of TiO₂ to that of PbS, though the VB of TiO₂ lies at a more positive potential. So, for PbS, its narrow band gap may work as electron traps capturing the excited electrons from TiO₂, thus enhanced the separation of photoproducted electrons and holes to some extent. On the other hand, after coupling with PbS, TiO₂/PbS nanotube arrays can absorb more visible-region light to generate more electrons and holes (Fig. 5a). Based on the two reasons, TiO₂/PbS nanotube arrays showed the better photocatalytic activity than the bare TiO₂ nanotube arrays.

As schematized in Fig. 6b, the CB of TiO₂ lies at a more positive potential than that of ZnS, while the VB of ZnS is more negative than that of TiO₂. For TiO₂/ZnS, excited electrons and holes will prefer to be collected by TiO₂ and ZnS, respectively. Such band structure facilitates the separation of the excited electron-hole pairs, therefore efficiently prevents the recombination of holes and electrons. Longer life-time of photogenerated electrons and holes ensures better photocatalytic performance of TiO₂/ZnS composite nanotubes than that of bare TiO₂ nanotubes.

It was reported that the structure of the samples had an effect on the light absorption of the catalysts²⁷⁻²⁹. In addition, the photocatalytic activity could be influenced by the thickness of MS layer or TiO₂ layer. But the main purpose of our work is to report a new method for preparing well-ordered arrays of TiO₂/MS(M=Pb,Zn) nanotubes and compare the difference of the photocatalytic activities with different structures. Further investigation about the factors such as the structure of the samples and the thickness of the layer will be shown in our future work.

In this study, through liquid deposition, the TiO₂/PbS and TiO₂/ZnS nanotube arrays were successfully synthesized by using AAO templates. TiO₂/PbS and TiO₂/ZnS nanotubes showed enhanced photocatalytic activities than bare TiO₂ nanotubes owing to their special band structures, which facilitated the separation of photogenerated holes and electrons. Method used to prepare the TiO₂/MS core-shell coaxial nanotube arrays is simple and convenient, and more composite materials with core-shell coaxial structure using the method could be expected in the future.

This work was financially supported by National Natural Science Foundation of China (Grant No. 51272115) and The

Scientific Research Encouragement Foundation for Outstanding Young and Middle Aged Scientists of Shandong Province, China (Grant No.BS2013CL025).

Notes and references

- ^aCollege of Materials Science and Engineering, Qingdao University of Science and Technology, Zhengzhou Road 53, Qingdao, 266042, China *E-mail address: dufanglin2008@hotmail.com Tel: +86-532-84022870
- ^bInstitute of Materials Science and Engineering, Ocean University of China, Songling Road 238, Qingdao 266100, China
- S. Guldin, P. Docampo, M. Stefik, G. Kamita, U. Wiesner and H. J. Snaith, U. Steiner, *small*, 2012, **8** (3), 432.
 - X. J. Xu, X. S. Fang, T. Y. Zhai, H. B. Zeng, B. D. Liu, X. Y. Hu, Y. S. Bando and D. Golberg, *small*, 2011, **7** (4), 445.
 - Z. F. Liu, K. Y. Guo, J. H. Han, Y. J. Li, T. Cui, B. Wang, J. Ya and C. L. Zhou, *small*, 2014, **10** (15), 3153.
 - X. L. Cui, M. Ma, W. Zhang, Y. C. Yang and Z. J. Zhang, *Electrochem. Commun.*, 2008, **10**, 367.
 - N. T. Nguyen, J. E. Yoo, M. Altomarea and P. Schmuki, *Chem. Commun.*, 2014, **50**, 9653.
 - S. Rühle, M. Shalom and A. Zaban, *Chem. Phys. Chem*, 2010, **11**, 2290.
 - F. Xu, X. Ma, C. R. Haughn, J. Benavides, M. F. Doty and S. G. Cloutier, *ACS NANO*, 2011, **5** (12), 9950.
 - Q. Kang, S. H. Liu, L. X. Yang, Q. Y. Cai, C. A. Grimes, *ACS Appl. Mater. Interfaces*, 2011, **3**, 746.
 - Y. L. Lee, C. F. Chi and S. Y. Liau, *Chem. Mater.*, 2010, **22**, 922.
 - C. Ratanatawanate, A. Chyao and K. J. Balkus, Jr., *J. Am. Chem. Soc.*, 2011, **133**, 3492.
 - K. Shin, S. I. Seok, S. H. Im and J. H. Park, *Chem. Commun.*, 2010, **46**, 2385.
 - V. Galstyan, A. Vomiero, I. Concina, A. Braga, M. Brisotto, E. Bontempi, G. Faglia and G. Sberveglieri, *small*, 2011, **7**(17), 2437.
 - T. Kasuga, M. Hiramatsu, A. Hoson, T. Sekino and K. Niihara, *Adv. Mater.*, 1999, **11** (15), 1307.
 - J. J. Qiu, Z. G. Jin, Z. F. Liu, X. X. Liu, G. Q. Liu, W. B. Wu, X. Zhang and X. D. Gao, *Thin Solid Films*, 2007, **515**(5), 2897.
 - Z. F. Bian, J. Zhu, F. L. Cao, Y. N. Huo, Y. F. Lu and H. X. Li, *Chem. Commun.*, 2010, **46**, 8451.
 - A. Varghese, P. Ghosh and S. Datta, *J. Phys. Chem. C*, 2014, **118**, 21604.
 - J. H. Dai, Q. Liu, L. Wang, P. W. Wu, X. Huang, Z. B. Zhu and J. T. Tian, *Mater. Lett.*, 2013, **107**, 333.
 - K. P. Acharya, N. N. Hewa-Kasakarage, T. R. Alabi, I. Nemitz, E. Khon, B. Ullrich, P. Anzenbacher and M. Zamkov, *J. Phys. Chem. C*, 2010, **114**, 12496.
 - X. D. Yu, Q. Y. Wu, S. C. Jiang and Y. H. Guo, *Mater. Charact.*, 2006, **57**, 333.
 - K. P. Acharya, E. Khon, T. O'Conner, I. Nemitz, A. Klinkova, R. S. Khnazyer, P. Anzenbacher and M. Zamkov, *ACS NANO*, 2011, **5** (6), 4953.
 - B. Ding, Y. Wang, P. S. Huang, D. H. Waldeck and J. K. Lee, *J. Phys. Chem. C*, 2014, **118**, 1474.
 - D. D. Lin, H. Wu, R. Zhang, W. Zhang and W. Pan, *J. Am. Ceram. Soc.*, 2010, **93** (10), 3384.
 - B. V. Crist. Handbook of The Elements and Native Oxides, 1999 XPS International, Inc, 3408 Emerald Drive, Ames Iowa 50010 USA
 - W. Jang, D. Kim, J. Kim, B. K. Min, J. D. Kim and K. P. Yoo, *Chem. Mater.*, 2010, **22**, 4350.
 - X. Yang, H. T. Xue, J. Xu, X. Huang, J. Zhang, Y. B. Tang, T. W. Ng, H. L. Kwong, X. M. Meng and C. S. Lee, *ACS Appl. Mater. Interfaces.*, 2014, **6**, 9078.
 - S. H. Wang and S. Q. Zhou, *J. Hazard. Mater.*, 2011, **185**, 77.
 - C. J. Chang, S. T. Hung, *Thin Solid Films*, 2008, **517**, 1279.
 - D. Majumdar, S. Chatterjee, M. Dhar, S.K. Dutta and H. Saha, *Sol. Energ. Mat. & Sol. C.*, 2003, **77**, 51.
 - M. H. Hsu and C. J. Chang, *Int. J. Hydrogen. Energ.*, 2014, **39**, 16524.

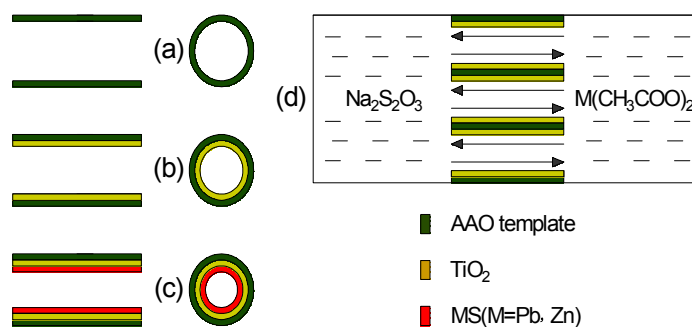
Fabrication of TiO₂/MS (M=Pb, Zn) core-shell coaxial nanotube arrays and their photocatalytic properties

Xiaofei Qu,^a Yuchen Hou,^a Chengpeng Wang,^a Fanglin Du^{*a} and Lixin Cao^b

^aCollege of Materials Science and Engineering, Qingdao University of Science and Technology, Zhengzhou Road 53, Qingdao, 266042, China

*E-mail address: dufanglin2008@hotmail.com Tel: +86-532-84022870

^bInstitute of Materials Science and Engineering, Ocean University of China, Songling Road 238, Qingdao 266100, China



TiO₂/MS (M=Pb, Zn) core-shell coaxial nanotube arrays were prepared by a simple method of liquid deposition, where the template worked as a septum.